COMMUNICATIONS

Electric field-controlled water permeation coupled to ion transport through a nanopore

J. Dzubiella,[a] R. J. Allen, and J.-P. Hansen
University Chemical Laboratory, Lensfield Road, Cambridge CB2 1EW, United Kingdom

(Received 30 October 2003; accepted 13 January 2004)

We report molecular dynamics simulations of a generic hydrophobic nanopore connecting two reservoirs which are initially at different Na^+ concentrations, as in a biological cell. The nanopore is impermeable to water under equilibrium conditions, but the strong electric field caused by the ionic concentration gradient drives water molecules in. The density and structure of water in the pore are highly field dependent. In a typical simulation run, we observe a succession of cation passages through the pore, characterized by approximately bulk mobility. These ion passages reduce the electric field, until the pore empties of water and closes to further ion transport, thus providing a possible mechanism for biological ion channel gating. © *2004 American Institute of Physics.* [DOI: 10.1063/1.1665656]

Water and ion permeation of nanopores is a key issue for biological membrane-spanning ion channels and aquaporins, as well as for materials like zeolites, gels and carbon nanotubes. Recent simulations report intermittent filling of hydrophobic nanopores by water under equilibrium conditions.[1–4] However, imbalances in ion concentrations between the inside and outside of cell membranes create strong electric fields.[5] Experiments on water near interfaces show that strong fields can induce considerable electrostriction of water.[6] The nonequilibrium behavior of confined water and ions in strong fields should therefore be very important for ion permeation and ion channel function. In particular, biological ion channels are known to ''open'' and ''close'' to ion transport in response to changes in the electric field across the membrane. This behavior, known as *voltage gating*, is crucial to their function, but despite recent experimental advances[7,8] its mechanism is so far not well understood.[5] Related theoretical approaches[9] to ion transport include the application of a uniform external electric field,[10,11] more specific models of particular proteins,[12–15] Brownian Dynamics[11] and continuum theories.[16] Here we present the results of MD simulations in which a strong electric field across the pore is explicitly created by an ionic charge imbalance, as is the case in a biological cell. We follow the relaxation of this nonequilibrium system to equilibrium.

Our generic model ion channel consists of a cylindrical pore of length $L_p = 15$ Å and radius $R_p = 5.5$ Å, through a membrane slab which separates two reservoirs containing water and Na^+ and Cl^- ions, as shown in Fig. 1. One reservoir has initial concentrations $c_{Na^+} \approx 0.9$ M (12 cations) and $c_{Cl^-} \approx 0.6$ M (8 anions), while for the second reservoir, $c_{Na^+} \approx 0.3$ M (4 cations) and $c_{Cl^-} \approx 0.6$ M (8 anions). This imbalance of charge generates an average electric field of 0.37 V/Å across the membrane. These ion concentrations and electric field are typically at least an order of magnitude larger than under ''normal'' physiological conditions, but they could be achieved in the course of a rare, large fluctuation at the pore entrance. Such a large initial ionic concentration gradient is necessary to improve the signal-to-noise ratio in the simulation. The chosen pore dimensions are comparable to those of the selectivity filter of a K^+ channel.[12,17]

Our simulation cell contains two of these pores in sequence along the z-axis, only one of which is shown in Fig. 1. The reservoir to the right of this pore thus forms the left reservoir for the other pore. Due to periodic boundary conditions, the right reservoir of the latter is also the left reservoir of the first. In this arrangement, which is the sim-

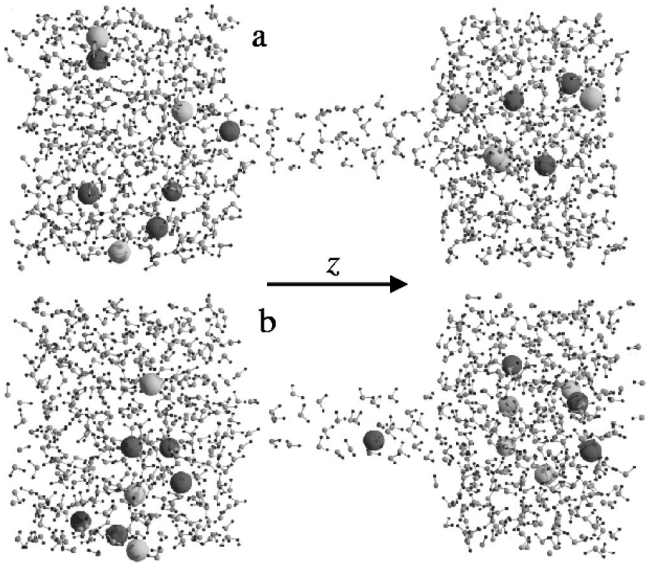

FIG. 1. Simulation snapshots. Molecular configurations (a) before a cation (dark gray spheres) permeates the channel and (b), 10 ps later, while it goes through. Anions are shown as light gray spheres. Only half of the periodically repeated simulation cell is shown.

[a]Electronic mail: jd319@cam.ac.uk

plest allowing the use of full three-dimensional periodic boundaries, the flow of ions in response to the concentration gradient will be antiparallel in the two channels. The relaxation towards equilibrium, where the two reservoirs are individually electroneutral, will thus involve an indirect coupling between the two pores.

The water molecules are modeled by the SPC/E potential[18] which consists of an O atom, carrying an electric charge $q=-0.8476e$, and two H atoms with $q=0.4238e$. The O atoms on different water molecules interact via a Lennard-Jones (LJ) potential with parameters $\epsilon=0.6502$ kJ mol^{-1} and $\sigma=3.169$ Å. The model is rigid, with OH bond length 1 Å and HOH angle 109.5°. The ion parameters used are those of Spohr.[19] The Na^+ ions have LJ parameters $\epsilon=0.3592$ kJ mol^{-1}, $\sigma=2.73$ Å and $q=+e$ while for Cl^-, $\epsilon=0.1686$ kJ mol^{-1}, $\sigma=4.86$ Å and $q=-e$.

Water O atoms interact with the membrane surfaces by a potential of the 9-3 form $V(z)=\epsilon'[(\sigma/z)^9-(\sigma'/z)^3]$, where z is the distance between the planar confining surface and the center of the O atom and $\epsilon'=5.031$ kJ/mol, $\sigma'=2.474$ Å. This potential is the same as that used for the study of liquid water between hydrophobic surfaces by Lee, McCammon, and Rossky[20] and is obtained by the integration of a water–hydrocarbon LJ interaction over an infinite wall. It is intended to mimic the interaction between a water molecule and a hydrocarbon surface. For the interaction between the particles and the interior cylindrical channel surface we used an analytical fit to the analogous integral over the volume surrounding an infinitely long pore. Linear interpolation procedures were applied at the pore edges to avoid any discontinuities. Very similar interactions were used in a previous work on water confined in pores, which revealed intermittent behavior of water permeation under equilibrium conditions.[3] Ion–water and ion–ion cross terms are defined using the usual Lorentz–Berthelot combining rules. Ions have the same form of interaction with the membrane surfaces as the water molecules, the parameters being $\epsilon'=4.928$ kJ/mol, $\sigma=3.078$ Å for the Cl^- and $\epsilon'=2.902$ kJ/mol, $\sigma'=2.317$ Å for the Na^+.

If R_p is the geometric radius of the cylindrical pore, one may conveniently define an effective radius R by the radial distance from the cylinder axis at which the interaction energy of a water O atom with the confining surface is zero, leading at room temperature to $R\approx R_p-2.5$ Å; similarly the effective length of the pore is $L\approx L_p+5.0$ Å. In order to verify that the striking behavior described below is not overly sensitive to details of the wall–particle interactions, we have also carried out simulations based on a Lennard-Jones 12-6 (rather than 9-3) interaction between the water and surfaces with the same effective pore radii and lengths. The results showed no qualitative changes; only slight differences of the water density profiles in the channel and at the membrane wall were observed. Polarizability of the membrane is neglected here. Earlier simulations[21] under equilibrium conditions showed that polarization effects are small, only slightly shifting the transition from closed to intermittent states of the pore.

The total simulation cell including both channels is of dimensions $l_x=l_y=23.5\pm0.3$ Å and $l_z=114.3\pm1.7$ Å and contains 1374 water molecules, 16 Na^+ and 16 Cl^- ions. Molecular dynamics simulations were carried out with the DLPOLY2 package,[22] using the Verlet algorithm[23,24] with a timestep of 2 fs. The pressure was maintained at $P=1$ bar and the temperature at $T=300$ K using a Berendsen barostat and thermostat.[25] Electrostatic interactions were calculated using the particle–mesh Ewald method.[26]

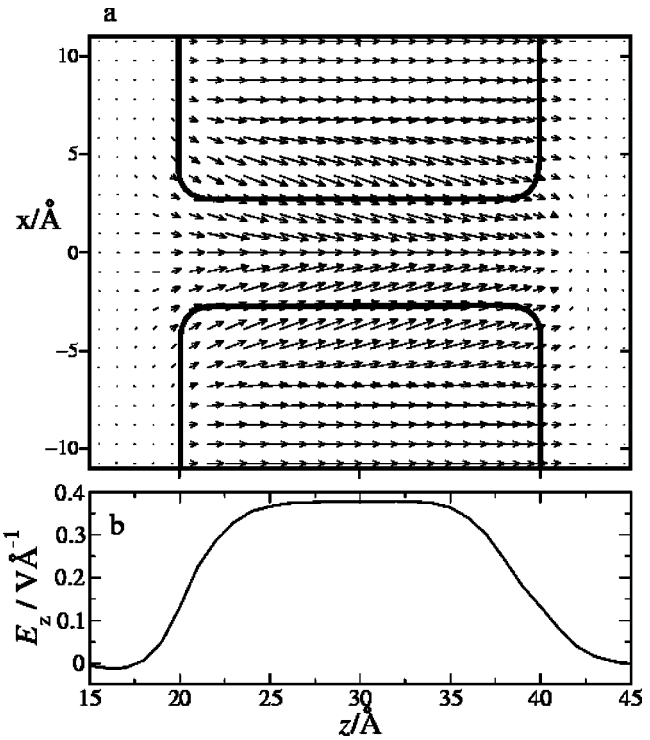

FIG. 2. Electric field in and around the pore before the first ion crossing. (a) Magnitude and direction of the electric field, depicted by vectors on a two-dimensional rectangular grid in the x-z plane. The contour of the membrane pore is sketched as black solid line. (b) Averaged z-component $E_z(z)$ of the electric field inside the channel.

The striking result of these simulations is that permeation of the pore by water is strongly affected by the electric field. The effective channel radius chosen for most of the simulations ($R\approx3$ Å) is such that under equilibrium conditions (i.e., with equal numbers of anions and cations on both sides and hence no electric field), the channel is empty of water and ions as demonstrated in previous work[3] and verified for the present simulation cell. However, under nonequilibrium conditions, the ionic charge imbalance across the membrane causes the pore to fill spontaneously with water. The electric field throughout the system was monitored by measuring the electrostatic force on phantom test particles on a three dimensional grid.[10] Figure 2(a) shows the average local electric field around one pore before the first ion moves through a channel. It is nearly zero in the reservoirs. Inside the pore the field is very strong (~0.37 V/Å) and has a small inward radial component. The profile of the z-component of the field E_z is shown in Fig. 2(b) and is constant inside the pore.

During the course of the simulation, a number of Na^+ ions move through the pore. Each of these events changes the reservoir charge imbalance and reduces the electric field in the pore. This has a dramatic effect on the behavior of the

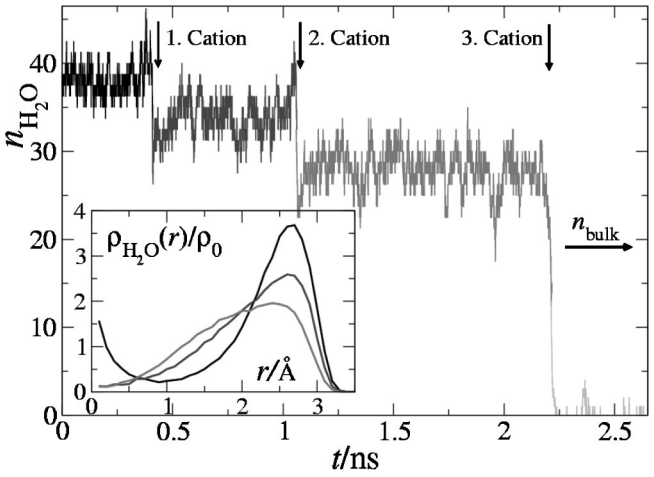

FIG. 3. Occupancy and structure of water inside the pore. The number of water molecules inside the channel n_{H_2O} is plotted as a function of time t. The shades of gray code the average magnitude of the electric field inside the pore: from black to light gray: $E \approx 0.37$ V/Å, $E \approx 0.26$ V/Å, $E \approx 0.15$ V/Å, $E \approx 0.10$ V/Å. The inset shows the corresponding radial density profiles of the water molecules inside the channel averaged over periods of constant field. ρ_0 is the bulk density of water in equilibrium. n_{bulk} [Eq. (1)] is the expected number of water molecules inside the pore if bulk density is assumed.

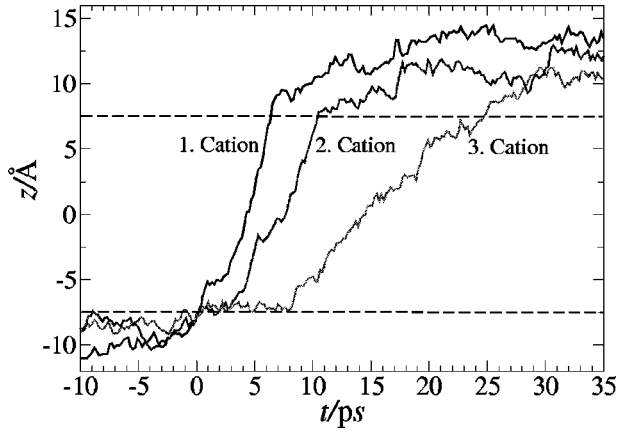

FIG. 4. Cation trajectories inside the pore and in its vicinity. The z-coordinate of the cations is plotted versus time for three successive permeations in one typical simulation run. The cylindrical pore is located between $z=-7.5$ Å and $z=7.5$ Å marked by the two long dashed lines. $t=0$ defines the time at which the ions are located at the entrance of the pore. The shades of gray code the average magnitude of electric field experienced by the ions, as in Fig. 3.

water, as shown in Fig. 3 in which the number n_{H_2O} of water molecules inside one pore is plotted as a function of time for a typical simulation run.

Initially, the water in the pore undergoes strong electrostriction, comparable to experimental observations.[6] If the average density in the pore is defined by $\rho \approx n_{H_2O}/(\pi R^2 L)$, then ρ is twice as large as that of bulk water in equilibrium. If we assume bulk density of water ρ_0 inside a channel of radius R and length L we expect an average number n_{bulk} of molecules inside the channel with

$$n_{bulk} = \rho_0(\pi R^2 L). \tag{1}$$

n_{bulk} is indicated with an arrow on the right-hand side in Fig. 3. At each ion crossing, the number n_{H_2O} of water molecules inside the pore drops but is still larger than n_{bulk}. In the particular simulation run shown in Fig. 3 three cations pass through this pore. After the third ion crosses ($t \approx 2.23$ ns), the electric field is no longer strong enough to sustain channel filling and the pore spontaneously empties of water, thereby becoming impermeable to further ion transport. However the other pore in the simulation cell remains filled and the final ion crossing eventually occurs through this pore which thereafter also empties of water. At this stage, the system has returned to equilibrium and both channels are empty of water. On repeating the simulation 10 times with different initial conditions, we observe that the closing of one pore after the third ion passes through it occurs in all runs.

We believe that the presence of water within the channel is critical for an ion to enter. When the channel is empty of water, the sodium ion experiences a large potential barrier at the entrance; this can be approximated by the solvation free energy in water ($\Delta G \approx 347$ kJ/mol).[27] If we assume a constant electric field and a typical distance d over which the ion with charge q sheds its solvation shell while entering the empty pore (roughly its diameter $d \approx 3$ Å) the field to overcome the energy barrier must be about $E = \Delta G/(qd) \approx 1.2$ V/Å, which is one order of magnitude higher than the fields observed for our parameters when the channel empties of water. Since the electric field is even smaller at the pore entrance than in the pore center we expect that only unreasonably high fields could drive ions through an empty pore. Obviously, the energy barrier for the ion to enter an empty channel will be smaller when polarizability of the membrane is included, or when polar groups are added on the surface of the channel. In the present simulations we never observed an isolated ion crossing an empty pore.

The structure of water in the filled pore is strongly affected by the field, as shown in the inset of Fig. 3. Before the first ion crossing, water forms clear-cut layers near the pore wall and along the z-axis. The central layer disappears after the first ion crossing and the outer layer becomes less well-defined. After a further ion crossing, water is more evenly distributed, as observed in the equilibrium simulations of Allen *et al.*[3]

Ion transport through the pore is found to occur essentially at constant velocity. Figure 1 shows snapshots from a typical simulation run just before (a) and while (b) a sodium ion passes through the channel. Within the reservoirs the anions and cations diffuse among the water molecules. When a cation in the Na^+-rich reservoir comes close to the channel entrance, it experiences the strong axial field shown in Fig. 2 and is dragged into the channel. Analysis of the ion passages for ten simulation runs, with the same initial charge imbalance but different initial configurations, shows that once an ion enters the channel, it moves mainly with a constant velocity which is approximately the same in all runs, and then reverts to diffusive motion in the reservoir at the other end of the channel.

Figure 4 shows typical cation positions along the z-axis, as a function of time, for the first, second and third ion crossings, as shown in Fig. 3. The velocity of an ion traversing the pore decreases with the number of previous cation crossings

due to the lowering of the driving electric field. It appears that the second and third ion pause for a few ps at the channel entrance, perhaps in order to shed their bulklike solvation shell. We observe that this ''pausing time'' is rather widely distributed between simulation runs. The cation mobility μ_+, defined by $\mathbf{v}=\mu_+ e\mathbf{E}$, can be calculated from the slopes of the trajectories in Fig. 4, together with the measured electric fields, as in Fig. 2. The resulting values are $\mu_+ \approx 4.5 \times 10^{11}\,\mathrm{s\,kg^{-1}}$ for the first ion, $\mu_+ \approx 3.8\times 10^{11}\,\mathrm{s\,kg^{-1}}$ for the second ion, and $\mu_+ \approx 2.4\times 10^{11}\,\mathrm{s\,kg^{-1}}$ for the third ion, averaged each over data from 10 simulations runs with different initial configurations. These values are close to the value of $\mu_+ \approx 2.3\times 10^{11}\,\mathrm{s\,kg^{-1}}$ obtained from the self-diffusion constant in the reservoir D_+, using Einstein's relation $\mu_+ = D_+ / k_B T$, but seem to increase with the magnitude of the electric field inside the pore. This enhancement of the mobility correlates with the change of structure of the water inside the channel, shown in the inset of Fig. 3. The tetrahedral hydrogen bond network which water forms under equilibrium conditions is disrupted inside the pore under high electric fields.

In order to test the effect of increasing the box size in the lateral directions we doubled the box area in the x-y plane, keeping the ion concentration gradient constant. As a consequence the number of water molecules and ions was doubled as well, and so twice the number of ion passages were required before the system relaxed to equilibrium. The jumps in the macroscopic electric field and in the number of water molecules inside the channel during an ion passage are thus smaller in this case than those shown in Fig. 3.

Changes of the pore radius or length give qualitatively the same results, apart from the fact that for pore radii larger than $R \approx 5$ Å the pore is always filled with water.[3] For smaller radii the critical electric field for water permeation is, however, sensitive to the pore radius and length. This suggests that voltage-dependent gating in ion channels, if it were to occur through changes in water permeation of a hydrophobic section of the pore,[2–5] might be strongly dependent on channel geometry.

The key finding which emerges from our simulations is the strong correlation between water and ion behavior in a simple pore under nonequilibrium conditions. Ionic charge imbalance across the membrane induces water permeation of the hydrophobic pore and thus makes it permeable to ions. This suggests that voltage gating of ion channels could be linked to the coupling between water and ion permeation in pores far from equilibrium. The structure and density of water in the pore is dramatically affected by the strong electric field in a way which is insensitive to the details of the confining potential or the simulation box size. In our simulation runs, the passage of a cation through the channel causes an abrupt jump of the electric field, and an ensuing jump in the number of water molecules inside the pore. Ion passage through the pore occurs at constant velocity and with a mobility coefficient similar to that of the bulk solution at equilibrium.

The authors are grateful to Jane Clarke and Michele Vendruscolo for a careful reading of the manuscript. This work was supported in part by the EPSRC. R.J.A. is grateful to Unilever for a Case award.

[1] G. Hummer, J. C. Rasaiah, and J. P. Nowortya, Nature (London) **414**, 188 (2001).
[2] O. Beckstein, P. C. Biggin, and M. S. P. Sansom, J. Phys. Chem. B **105**, 12902 (2001).
[3] R. Allen, S. Melchionna, and J.-P. Hansen, Phys. Rev. Lett. **89**, 175502 (2002); J. Chem. Phys. **119**, 3905 (2003).
[4] O. Beckstein and M. S. P. Sansom, Proc. Natl. Acad. Sci. U.S.A. **100**, 7063 (2003).
[5] B. Hille, *Ionic Channels of Excitable Membranes* (Sinauer, Sunderland, MA, 1992).
[6] M. F. Toney, Nature (London) **368**, 444 (1994).
[7] Y. Jiang, A. Lee, J. Chen, M. Cadene, B. T. Chait, and R. MacKinnon, Nature (London) **417**, 523 (2002).
[8] Y. Jiang, A. Lee, J. Chen, V. Ruta, M. Cadene, B. T. Chait, and R. MacKinnon, Nature (London) **423**, 33 (2003).
[9] S. Kuyucak, O. S. Andersen, and S.-H. Chung, Rep. Prog. Phys. **64**, 1427 (2001).
[10] P. S. Crozier, R. L. Rowley, N. B. Holladay, D. Henderson, and D. D. Busath, Phys. Rev. Lett. **86**, 2467 (2001).
[11] S.-H. Chung, T. W. Allen, and S. Kuyucak, Biophys. J. **83**, 263 (2002).
[12] S. Bernèche and B. Roux, Nature (London) **414**, 73 (2001).
[13] D. P. Tieleman, P. C. Biggin, G. R. Smith, and M. S. P. Sansom, Quart. Rev. Biophys. **34**, 473 (2001).
[14] B. Roux and M. Karplus, Annu. Rev. Biophys. Biomol. Struct. **23**, 731 (1994).
[15] C. F. Lopez, M. Montal, J. K. Blasie, M. L. Klein, and P. B. Moore, Biophys. J. **83**, 1259 (2002).
[16] W. Nonner and B. Eisenberg, Biophys. J. **75**, 1287 (1998).
[17] Y. Zhou, J. H. Morais-Cabral, A. Kaufman, and R. MacKinnon, Nature (London) **414**, 43 (2001).
[18] H. J. C. Berendsen, J. R. Grigera, and T. P. Straatsma, J. Phys. Chem. **91**, 6269 (1987).
[19] E. Spohr, Electrochim. Acta **44**, 1697 (1999).
[20] C. Y. Lee, J. A. McCammon, and P. J. Rossky, J. Chem. Phys. **80**, 4448 (1984).
[21] R. Allen, S. Melchionna, and J.-P. Hansen, J. Phys.: Condens. Matter **15**, S297 (2003).
[22] W. Smith and T. R. Forester (1999), the DLPOLY_2 User Manual.
[23] D. Frenkel and B. Smit, *Understanding Molecular Simulation: From Algorithms to Applications*, 2nd ed. (Academic, New York, 2001).
[24] M. P. Allen and D. J. Tildesley, *Computer Simulation of Liquids* (Clarendon, Oxford, 1987).
[25] H. J. C. Berendsen, J. P. M. Postma, W. F. van Gunsteren, A. DiNola, and J. R. Haak, J. Chem. Phys. **81**, 3684 (1984).
[26] U. Essmann, L. Perera, M. L. Berkowitz, T. Darden, H. Lee, and L. G. Pedersen, J. Chem. Phys. **103**, 8577 (1995).
[27] R. M. Lynden-Bell and J. C. Rasaiah, J. Chem. Phys. **107**, 1981 (1997).